Supporting Information

Green, efficient and controllable synthesis of high-quality MOF-74 with high gravity technology

Xin-Ran Shi[a,b], Meng Qiao[a,b], Yan Wei[b,c], Ling-Xia Yun[a,b], Jie-Xin Wang[a,b],*, Jian-Feng Chen[a,b]

[a]State Key Laboratory of Organic-Inorganic Composites, Beijing University of Chemical Technology, Beijing 100029, PR China;

[b]Research Center of the Ministry of Education for High Gravity Engineering and Technology, Beijing University of Chemical Technology, Beijing, 100029, PR China

[c]China Chengda Engineering Co.Ltd, Chengdu, 610041, China

Total number of pages: 18

Total number of Fig.s:11 (Fig.s S1-S11)

Total number of Tables:5 (Table S1-S5)

* Corresponding authors:
Jie-Xin Wang, E-mail: wangjx@mail.buct.edu.cn (J.X. Wang)

Synthesis of MOF-74

MOF-74-Co-227 nm: The preparation process was consistent with MOF-74-Co-78 nm except that no acetic acid was added to the precursor.

MOF-74-Co-1.86 μm: The preparation process was consistent with MOF-74-Co-227 nm except that the reaction temperature is 70℃.

MOF-74-Zn: $Zn(OAc)_2$ (2.0 g, 10.8 mmol) were dissolved in 30 mL deionized water to obtain the metal salt precursor solution, dhtp (1.07 g, 5.4 mmol) and NaOH (0.86 g, 21.6 mmol) were dissolved in 200 mL of deionized water to obtain the ligand precursor solution. The molar ratio of the reactants (Zn/dhtp/NaOH) is 2:1:4. Two streams of precursor solutions were pumped into RPB through peristaltic pumps at a flow rate of 100 mL min^{-1}, respectively. Precursors are well mixed in RPB under the rotating speeds of 1500 rpm to achieve rapid nucleation and crystallization processes at room temperature. The product is collected immediately at the outlet. MOF-74-Zn was centrifuged out of the suspension, washed three times in deionized water and methanol respectively, and then dried for 12 h at 70℃.

MOF-74-Ni: $Ni(OAc)_2 \cdot 4H_2O$ (2.68 g, 10.8 mmol) were dissolved in 30 mL deionized water to obtain the metal salt precursor solution, dhtp (1.07 g, 5.4 mmol) and NaOH (0.86 g, 21.6 mmol) were dissolved in 200 mL of deionized water to obtain the ligand precursor solution. The molar ratio of the reactants (Ni/dhtp/NaOH) is 2:1:4. The following process is consistent with the MOF-74-Co preparation process.

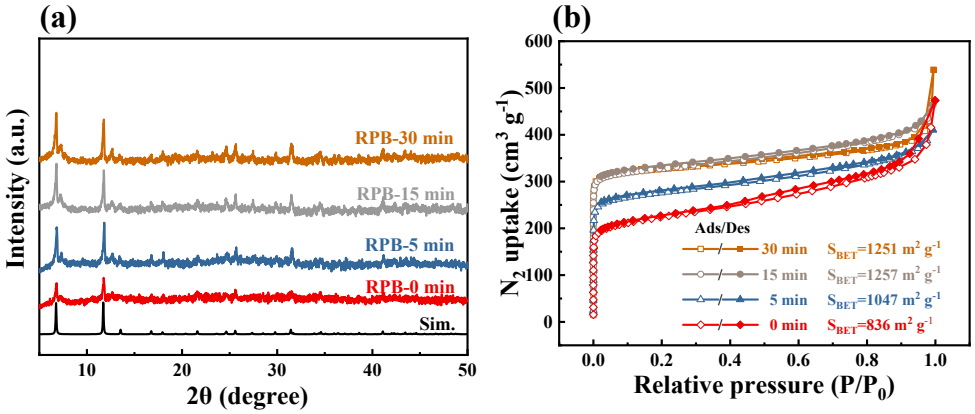

Figure S1. XRD patterns and N_2 adsorption-desorption isotherms of MOF-74-Co prepared in RPB under different reaction times.

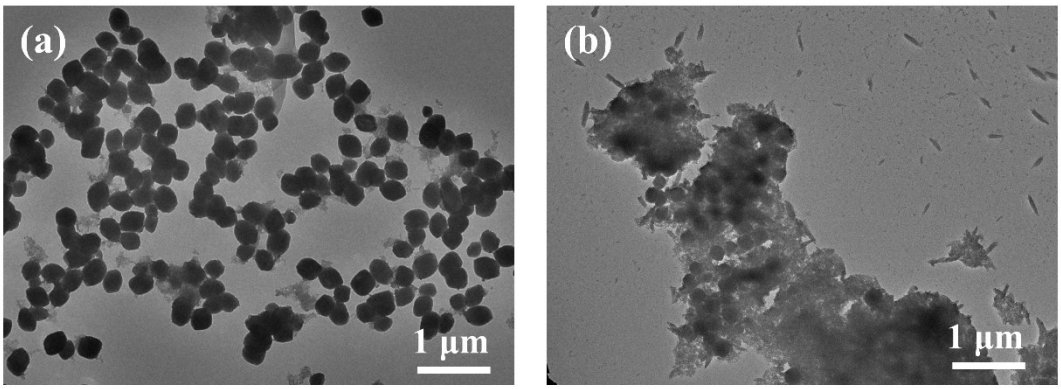

Figure S2. TEM images of MOF-74-Co (a) prepared by continuous stirring in STR for 30 min, (b) prepared by stirring in STR for 10 s then left to stand for 30 min.

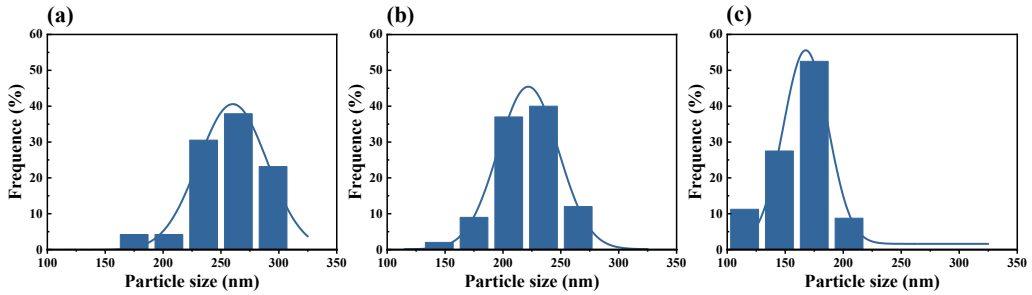

Figure S3. Particle size distributions of MOF-74-Co synthesized in RPB: (a) 500 rpm, (b) 1500 rpm, (c) 2500 rpm.

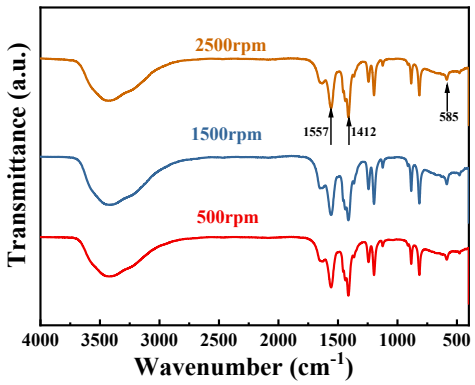

Figure S4. FTIR spectra of MOF-74-Co prepared at different rotating speeds.

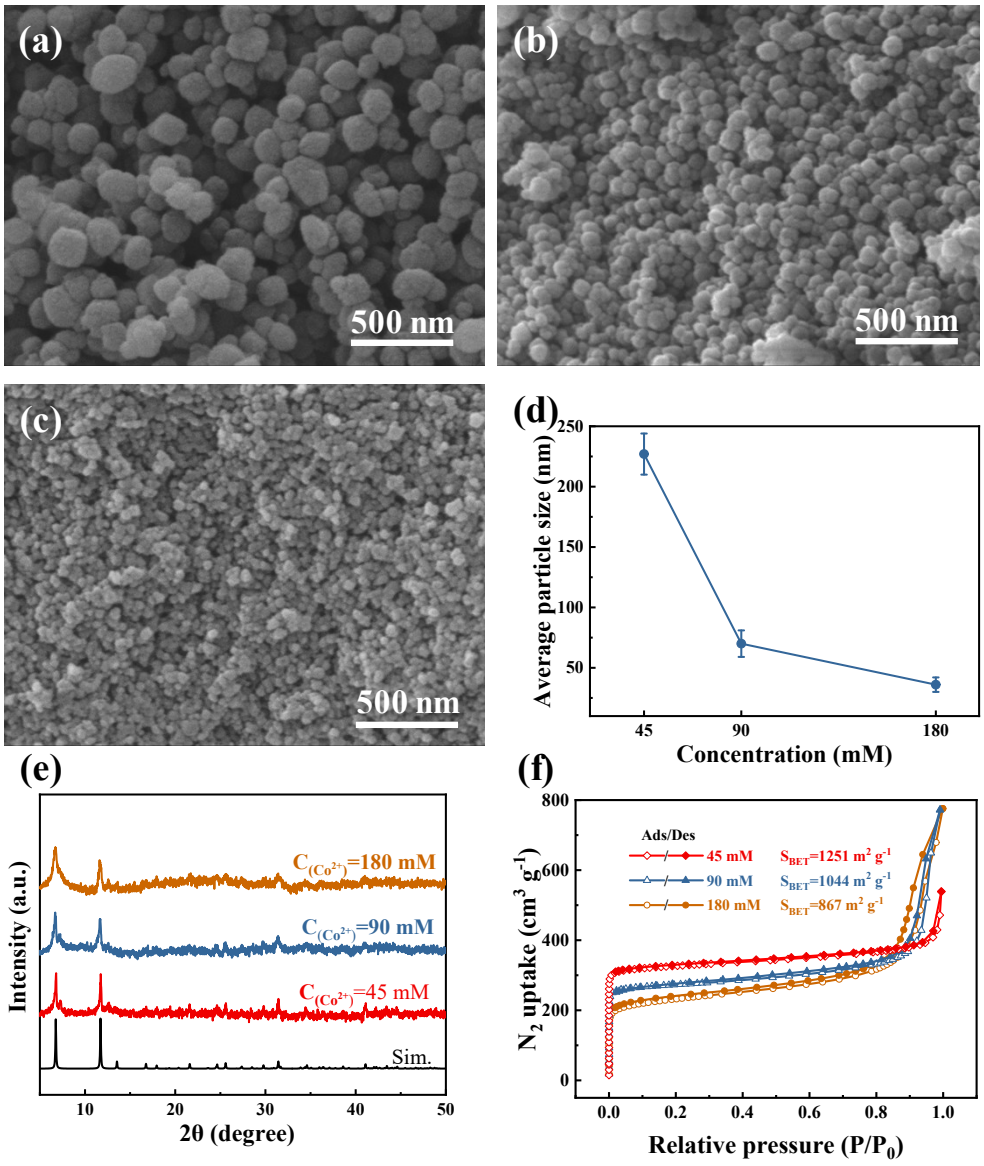

Figure S5. SEM images of the MOF-74-Co synthesized at different concentrations of precursors (molar ratio of Co/dhtp/NaOH = 2/1/4): (a) $C_{(Co)}$ =45 mM, (b) $C_{(Co)}$ =90 mM, (c) $C_{(Co)}$ =180 mM. (d) The average particle sizes, (e) XRD patterns, (f) N_2 adsorption-desorption isotherms of the MOF-74-Co synthesized at different concentrations of precursors.

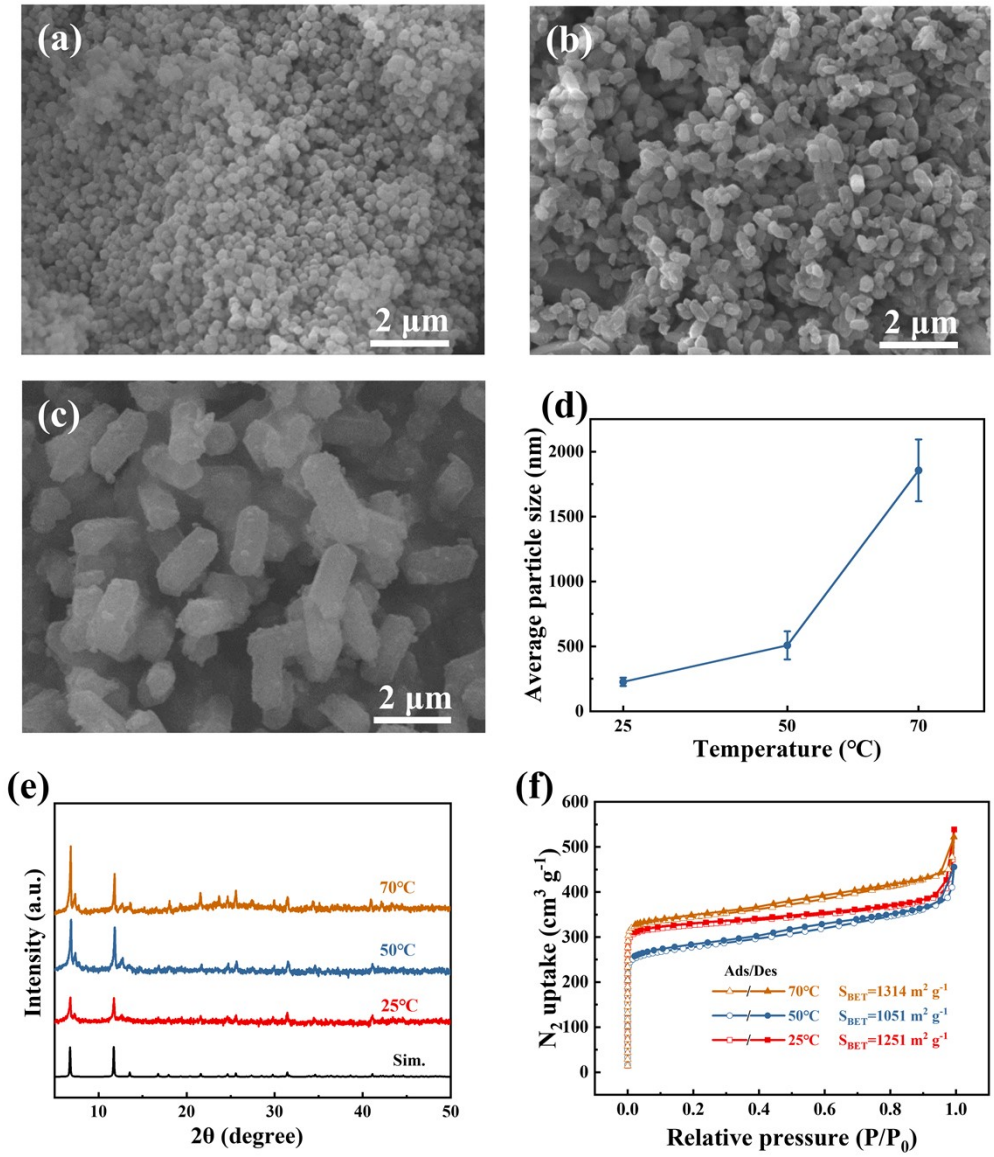

Figure S6. The SEM images of MOF-74-Co synthesized at different temperatures: (a) 25°C, (b) 50°C, (c) 70°C. (d) The average particle sizes (length), (e) XRD patterns, (f) N_2 adsorption-desorption isotherms of the MOF-74-Co synthesized at different temperatures.

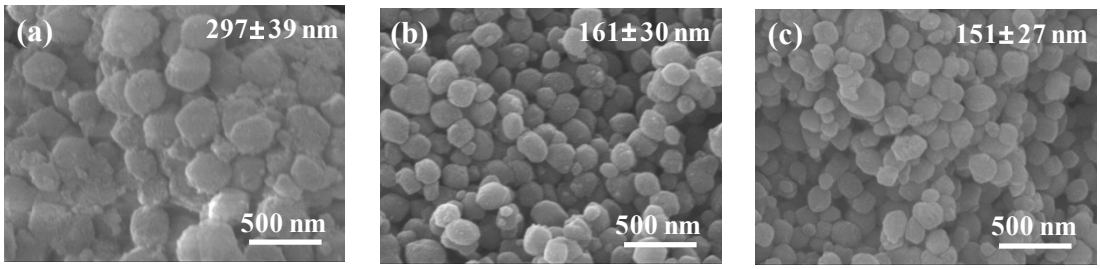

Figure S7. SEM images of MOF-74-Co synthesized under different additions of acetic acid in STR: (a) Without acetic acid, (b) 0.23 equiv acetic acid, (c) 0.46 equiv acetic acid.

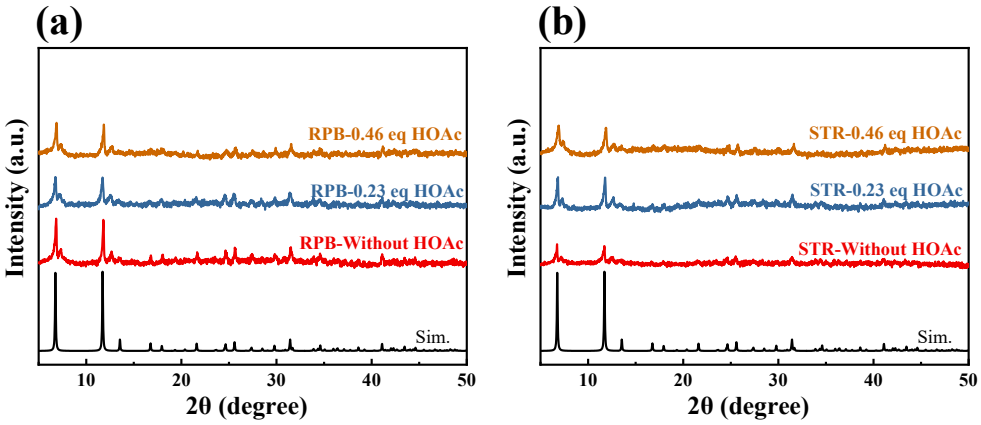

Figure S8. XRD patterns of MOF-74-Co synthesized under different additions of acetic acid: (a) RPB, (b) STR.

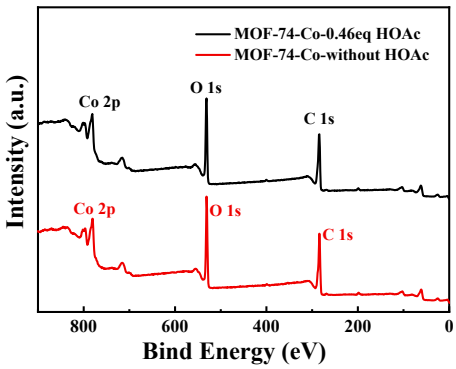

Figure S9. XPS spectra of MOF-74-Co-without HOAc and MOF-74-Co-0.46 eq.

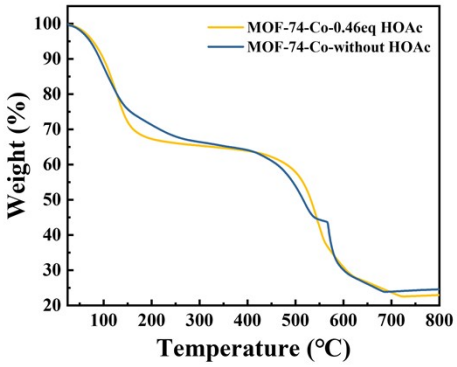

Figure S10. TG curves of MOF-74-Co-0.46eq HOAc and MOF-74-Co-without HOAc in an air atmosphere.

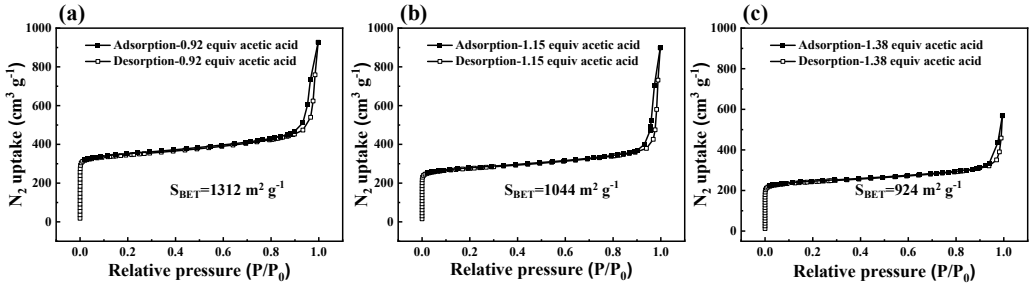

Figure S11. N_2 adsorption-desorption isotherms at 77 K of MOF-74-Co obtained at excessive additions of acetic acid: (a) 0.92 equiv acetic acid, (b) 1.15 equiv acetic acid, (c) 1.38 equiv acetic acid.

Table S1. Comparison of reaction conditions, particle sizes and BET surface areas of reported MOF-74-Co.

Samples	Solvent	Reaction time	Reaction temperature	Particle sizes	BET ($m^2 g^{-1}$)	Refs
MOF-74-Co	Water	30 min	RT	78 nm	1599	**This work**
a1	Water	24 h	RT	50±5 nm	1572	1
a2	Water	1 h	RT		962	1
b	Water	20 h	RT	5.1 nm	521	2
c	DMF/ethanol/H_2O	24 h	125℃		1080	3
d	DMF/ethanol/H_2O	24 h	100℃	＞50 μm	1007	4
e1	DMF/ethanol/H_2O	1 h	130℃	50 μm × 8 μm	1314	5
e2	DMF/ethanol/H_2O	24 h	100℃	300 μm ×70 μm	1327	5
f	water /THF	3 day	110℃	-	1284	6
g	DMF/ethanol/H_2O	18 h	125℃	-	1438	7
h	methanol	20 h	RT	-	925	8
i	DMF/ethanol/H_2O	24 h	100℃	-	502	9

Table S2. Comparison of synthesis condition, BET surface areas, STY and yield of MOFs using green synthesis methods.

Methods	MOFs	Solvent	Temperature (℃)	Time (h)	BET ($m^2 g^{-1}$)	STY (kg m^{-3} day^{-1})	Yield (%)	Refs
High-gravity	MOF-74-Co-0 min	water	RT[a]	0.033[b]	836	4156	81	**This work**
	MOF-74-Co-78nm			0.53[b]	1599	293	91	**This work**
Stirred tank reactor	MOF-74-Co	water	RT	1	962	1462	90	1
				24	1572	16	93	
	ZIF-93	water	RT	18	604	14	79	10
	HKUST-1	water	RT	12	1577	64	90	11
				0.5	930	2366	94	
	MIL-100	water	RT	24	1974	-	76	12
Stirred Reflux	MOF-74-Ni	water	160	1	1355	680	92	13
	MIL-160(Al)	water	100-150	24	1150	185	93	14
Centrifuge	UiO-66	water	RT	0.167	339	2732	79	15
Microwave	MOF-808	water	100	2	2050	-	-	16
Mechano-synthesis	MIL-100(Al)	Solvent-Free	240	18	1090	-	89	17
	UiO-66	Solvent-Free	130	12	1115	-	92	18
	$Cd_2(BTC)_3$	Solvent-Free	RT	0.167	64	1.44×10^6	82.5	19
	MIL-100-Cr	Solvent-Free	220	15	1848	-	22	20
	MOF-808	Solvent-Free	RT	1	702	15 g/h	-	21

[a]RT: Room temperature

[b] time = feed time + synthesis time

Table S3. Comparison of reaction conditions, particle sizes and BET surface areas of reported MOF-74-Zn.

MOFs	Solvent	Reaction time	Reaction temperature	Particle sizes	BET ($m^2 g^{-1}$)	Refs
MOF-74-Zn	Water	<1 s	RT	2.6×4.5 μm	1332	**This work**
	Water	5 min	RT		1154	1
	Water	10 min	RT	5.1×1.6 μm	1279	1
	DMF/H_2O	20 h	100℃		816	3
	Water	20 h	RT	3×1 μm	1039	22
	Tris buffer solution (pH 8.0)	10 min	RT	8 × 2 × 1 μm	174	23

Table S4. Comparison of reaction conditions, particle sizes and BET surface areas of reported MOF-74-Ni.

MOFs	Solvent	Reaction time	Reaction temperature	Particle sizes	BET ($m^2 g^{-1}$)	Refs
MOF-74-Ni	Water	30 min	RT	16 nm	1106	**This work**
	Water	6 h	RT	29 nm	1220	1
	Water	24 h	RT	-	1351	1
	Water	20 h	RT	2.8 nm	402	2
	DMF/ethanol/H_2O	24 h	100℃	-	1070	3
	Water	24 h	110℃	106 nm	1025	24
	H_2O/THF	24 h	67℃	33 nm	1081	24
	Water	1 h	80℃	1 μm	1233	13
	DMF/ethanol/H_2O	24 h	135℃	-	848	25

Table S5. Comparison of CO_2 adsorption capacity of different adsorbents.

Types of absorbents	Sample	CO_2 adsorption capacity (mg g^{-1})	Adsorption conditions	Refs
MOF	MOF-74-Co-78 nm	298	25℃,100 kpa	**This work**
	MOF-74-Co- 227 nm	245	25℃,100 kpa	**This work**
	MOF-74-Co- 1.86 μm	261	25℃,100 kpa	**This work**
	MOF-74-Co	256	25℃,100 kpa	3
	MOF-74-Co	288	25℃,100 kpa	5
	MOF-74-Co	210	25℃,100 kpa	5
	MOF-74-Co	304	25℃,100 kpa	6
	MOF-74-Co	304	25℃,100 kpa	7
	MOF-74-Co	107	45℃,100 kpa	26
	CALF-20	179	20℃,1.2 bar	27
	Aluminum Fumarate	55	35℃, 1 bar	28
	ZIF-8	66	25℃,100 kpa	29
	MIL-101(Cr)	101	25℃,100 kpa	30
	MIL-53(Al)	95	25℃,100 kpa	31
	UiO-66(Zr)	109	25℃,100 kpa	32
	NH_2-MIL-101(Al)	96	25℃,100 kpa	33
Zeolites	K-X	182	25℃,100 kpa	34
	Mg-X	211	25℃,100 kpa	34
	Ca-X	241	25℃,100 kpa	34
	Na-MER-2.3	176	25℃,100 kpa	35
	Rb-gismondine	132	25℃,100 kpa	36
	zeolite-13X	150	25℃,100 kpa	37
	FAU zeolite	107	25℃,100 kpa	38
Carbonaceous	Activated Carbon	79	25℃,100 kpa	39

materials	Activated Carbon fibers	251	25℃,100 kpa	40
	N-doped Carbon nanostructure (CPC)	255	25℃,100 kpa	41
	PANI−GO	58	25℃,100 kpa	42
	PANI−NSGO	56	25℃,100 kpa	42
Polymers	BINP-4	13	25℃,100 kpa	43
	hyper-cross-linked ionic polymers	121	0℃,100 kpa	44
	ADS-17	264	25℃,0.2 Mpa	45
	PIM-TPB-HSO3	179	25℃,100 kpa	46
	Ad-MALP-1	89	25℃,100 kpa	47
	TPPA–DMB	76	25℃,100 kpa	48

References

1 L. Garzón-Tovar, A. Carné-Sánchez, C. Carbonell, I. Imaz and D. Maspoch, *J. Mater. Chem. A*, 2015, **3**, 20819-20826.

2 M. Díaz-García, Á. Mayoral, I. Díaz and M. Sánchez-Sánchez, *Cryst. Growth Des.*, 2014, **14**, 2479-2487.

3 S. R. Caskey, A. G. Wong-Foy and A. J. Matzger, *J. Am. Chem. Soc.*, 2008, **130**, 10870-10871.

4 H. Jiang, Q. Wang, H. Wang, Y. Chen and M. Zhang, *ACS Appl. Mater. Interfaces*, 2016, **8**, 26817-26826.

5 H.-Y. Cho, D.-A. Yang, J. Kim, S.-Y. Jeong and W.-S. Ahn, *Catal. Today*, 2012, **185**, 35-40.

6 D. Yu, A. O. Yazaydin, J. R. Lane, P. D. C. Dietzel and R. Q. Snurr, *Chem. Sci.*, 2013, **4**, 3544-3556.

7 W. L. Queen, M. R. Hudson, E. D. Bloch, J. A. Mason, M. I. Gonzalez, J. S. Lee, D. Gygi, J. D. Howe, K. Lee, T. A. Darwish, M. James, V. K. Peterson, S. J. Teat, B. Smit, J. B. Neaton, J. R. Long and C. M. Brown, *Chem. Sci.*, 2014, **5**, 4569-4581.

8 J. G. Flores, M. Díaz-García, I. A. Ibarra, J. Aguilar-Pliego and M. Sánchez-Sánchez, *J. Solid State Chem.*, 2021, **298**, 122151.

9 X. Deng, L. Yang, H. Huang, Y. Yang, S. Feng, M. Zeng, Q. Li and D. Xu, *Small*, 2019, **15**, 1902287.

10 E. V. Ramos-Fernandez, A. Grau-Atienza, D. Farrusseng and S. Aguado, *J. Mater. Chem. A*, 2018, **6**, 5598-5602.

11 C. Duan, F. Li, L. Li, H. Zhang, X. Wang, J. Xiao and H. Xi, *CrystEngComm*, 2018, 20, 1057-1064.

12 K. Guesh, C. A. D. Caiuby, Á. Mayoral, M. Díaz-García, I. Díaz and M. Sanchez-Sanchez, *Cryst. Growth Des.*, 2017, **17**, 1806-1813.

13 S. Cadot, L. Veyre, D. Luneau, D. Farrusseng and E. Alessandra Quadrelli, *J. Mater. Chem. A*, 2014, **2**, 17757-17763.

14 A. Permyakova, O. Skrylnyk, E. Courbon, M. Affram, S. Wang, U. H. Lee, A. H. Valekar, F. Nouar, G. Mouchaham, T. Devic, G. De Weireld, J.-S. Chang, N. Steunou, M. Frère and C. Serre, *ChemSusChem*, 2017, **10**, 1419-1426.

15 L. Huelsenbeck, H. Luo, P. Verma, J. Dane, R. Ho, E. Beyer, H. Hall, G. M. Geise and G. Giri, *Cryst. Growth Des.*, 2020, **20**, 6787-6795.

16 L. González, R. Gil-San-Millán, J. A. R. Navarro, C. R. Maldonado, E. Barea and F. J. Carmona, *J. Mater. Chem. A*, 2022, **10**, 19606-19611.

17 J. Li, M. J. Hurlock, V. G. Goncharov, X. Li, X. Guo and Q. Zhang, *Inorg. Chem.*, 2021, **60**, 4623-4632.

18 G. Ye, D. Zhang, X. Li, K. Leng, W. Zhang, J. Ma, Y. Sun, W. Xu and S. Ma, *ACS Appl. Mater. Interfaces*, 2017, **9**, 34937-34943.

19 Z. Guo, Q. Zhang, Z. Cheng, Q. Liu, J. Zuo, B. Jin and R. Peng, *ACS Sustainable Chem. Eng.*, 2020, **8**, 4037-4043.

20 Y. Mao, H. Qi, G. Ye, L. Han, W. Zhou, W. Xu and Y. Sun, *Microporous Mesoporous Mater.*, 2019, **274**, 70-75.

21 C. Jin, S. Shi, S. Liao, S. Liu, S. Xia, Y. Luo, S. Wang, H. Wang and C. Chen, *Chem. Mater.*, 2023, **35**, 4489-4497.

22 M. Sánchez-Sánchez, N. Getachew, K. Díaz, M. Díaz-García, Y. Chebude and I. Díaz, *Green Chem.*, 2015, **17**, 1500-1509.

23 P.-H. Hsu, C.-C. Chang, T.-H. Wang, P. K. Lam, M.-Y. Wei, C.-T. Chen, C.-Y. Chen, L.-Y. Chou and F.-K. Shieh, *ACS Appl. Mater. Interfaces*, 2021, **13**, 52014-52022.

24 J. Guasch, P. D. C. Dietzel, P. Collier and N. Acerbi, *Microporous Mesoporous Mater.*, 2015, **203**, 238-244.

25 S. Xie, Q. Qin, H. Liu, L. Jin, X. Wei, J. Liu, X. Liu, Y. Yao, L. Dong and B. Li, *ACS Appl. Mater. Interfaces*, 2020, **12**, 48476-48485.

26 J. Tapiador, E. García-Rojas, P. López-Patón, G. Calleja, G. Orcajo, C. Martos and P. Leo, *J. Environ. Chem. Eng.*, 2023, **11**, 109497.

27 J.-B. Lin, T. T. T. Nguyen, R. Vaidhyanathan, J. Burner, J. M. Taylor, H. Durekova, F. Akhtar, R. K. Mah, O. Ghaffari-Nik, S. Marx, N. Fylstra, S. S. Iremonger, K. W. Dawson, P. Sarkar, P. Hovington, A. Rajendran, T. K. Woo and G. K. H. Shimizu, *Science*, 2021,**374**,1464-1469.

28 Y. Ding, L. Ma, F. Zeng, X. Zhao, H. Wang, X. Zhu and Q. Liao, *Energy*, 2023, **263**, 125723.

29 Z. Li, B. He and S. Tang, *CrystEngComm*, 2024, **26,** 70-79.

30 C. Chen, N. Feng, Q. Guo, Z. Li, X. Li, J. Ding, L. Wang, H. Wan and G. Guan, J*J. Colloid Interface Sci.*, 2018, **513**, 891-902.

31 L. Sun, M. Yin, Z. Li and S. Tang, *J. Ind. Eng. Chem.*, 2022, **112**, 279-286.

32 V. N. Le, T. K. Vo, K. S. Yoo and J. Kim, *Sep. Purif. Technol.*, 2021, 274, 119079.

33 M. Babar, M. Mubashir, A. Mukhtar, S. Saqib, S. Ullah, M. A. Bustam and P. L. Show, *Environ. Pollut.*, 2021, **279**, 116924

34 A. M. Najafi, F. Khorasheh, S. Soltanali and H. Ghassabzadeh, *Langmuir*, 2023, **39**, 15535-15546.

35 H. J. Choi, D. Jo, J. G. Min and S. B. Hong, *Angew. Chem. Int. Ed.*, 2021, **60**, 4307-4314.

36 H. J. Choi, J. G. Min, S. H. Ahn, J. Shin, S. B. Hong, S. Radhakrishnan, C. V. Chandran, R. G. Bell, E. Breynaert and C. E. A. Kirschhock, *Mater. Horizons*, 2020, **7**, 1528-1532.

37 J. Hedlund, G. Garcia, M. Balsamo, M. Zhou and J. Mouzon, *Sep. Purif. Technol.,* 2021, **277**, 119483.

38 Y. Zhou, Y. Li, X. Yuan, G. Hou, M. Chu, H. Kang, W. Qin and X. Wu, *Sep. Purif. Technol.*, 2023, **325**, 124729.

39 J. Wang, L. Huang, R. Yang, Z. Zhang, J. Wu, Y. Gao, Q. Wang, D. O'Hare and Z. Zhong, *Energy Environ. Sci.*, 2014, **7**, 3478-3518.

40 X. Li, Y. Jin, Q. Xue, L. Zhu, W. Xing, H. Zheng and Z. Liu, *J. CO_2 Util.*, 2017, **18**, 275-282.

41 J. Zhou, Z. Li, W. Xing, H. Shen, X. Bi, T. Zhu, Z. Qiu and S. Zhuo, *Adv. Funct. Mater.*, 2016, **26**, 7955-7964.

42 S. Rodríguez-García, R. Santiago, D. López-Díaz, M. D. Merchán, M. M. Velázquez, J. L. G. Fierro and J. Palomar, *ACS Sustainable Chem. Eng.*, 2019, **7**, 12464-12473.

43 M. Maruthapandi, L. Eswaran, R. Cohen, N. Perkas, J. H. T. Luong and A. Gedanken, *Langmuir*, 2020, **36**, 4280-4288.

44 C. Li, H. Cai, X. Yang, F. Liu, C. Yang, P. Chen, Z. Chen and T. Zhao, *J. CO_2 Util.*, 2022, **64**, 102203.

45 H. Yang, X. Wang, J. Liu, W. Liu, Y. Gong and Y. Sun, *Chem. Eng. J.*, 2022, **430**, 132899.

46 H. Zhou, C. Rayer, A. R. Antonangelo, N. Hawkins and M. Carta, *ACS Appl. Mater. Interfaces*, 2022, **14**, 20997-21006.

47 M. Rong, L. Yang, C. Yang, J. Yu and H. Liu, *Microporous Mesoporous Mater.*, 2021, **323**, 111206.

48 E. Cucu, E. Dalkılıç, R. Altundas and A. E. Sadak, *Microporous Mesoporous Mater.*, 2022, **330**, 111567.